Published in final edited form as:

Neuroradiology. 2022 February ; 64(2): 217–232. doi:10.1007/s00234-021-02821-9.

Edited magnetic resonance spectroscopy in the neonatal brain

Yulu Song[1,2], **Peter J. Lally**[3], **Maria Yanez Lopez**[4], **Georg Oeltzschner**[1,2], **Mary Beth Nebel**[5,6], **Borjan Gagoski**[7,8], **Steven Kecskemeti**[9], **Steve C. N. Hui**[1,2], **Helge J. Zöllner**[1,2], **Deepika Shukla**[10], **Tomoki Arichi**[4,11], **Enrico De Vita**[4,12], **Vivek Yedavalli**[13], **Sudhin Thayyil**[10], **Daniele Fallin**[14,15], **Douglas C. Dean III**[9,16,17], **P. Ellen Grant**[7,8,18], **Jessica L. Wisnowski**[19,20], **Richard A. E. Edden**[1,2,13]

[1]Russell H. Morgan Department of Radiology and Radiological Science, The Johns Hopkins University School of Medicine, Baltimore, MD, USA

[2]F. M. Kirby Research Center for Functional Brain Imaging, Kennedy Krieger Institute, Baltimore, MD, USA

[3]Department of Brain Sciences, Imperial College London, London, UK

[4]Center for the Developing Brain, School of Biomedical Engineering and Imaging Sciences, King's College London, London, UK

[5]Center for Neurodevelopmental and Imaging Research, Kennedy Krieger Institute, Baltimore, MD 21205, USA

[6]Department of Neurology, Johns Hopkins University School of Medicine, Baltimore, MD, USA

[7]Department of Radiology, Division of Neuroradiology, Boston Children's Hospital, Harvard Medical School, Boston, MA, USA

[8]Fetal Neonatal Neuroimaging and Developmental Science Center, Boston Children's Hospital, Boston, MA, USA

[9]Waisman Center, University of WI–Madison, Madison, WI 53705, USA

[10]Centre for Perinatal Neuroscience, Department of Brain Sciences, Imperial College London, London, UK

[11]Department of Bioengineering, Imperial College London, South Kensington Campus, London, UK

[12]Biomedical Engineering Department, School of Biomedical Engineering and Imaging Sciences, St Thomas's Hospital, Westminster Bridge Road, Lambeth Wing, 3rd Floor, London SE1 7EH UK

✉Richard A. E. Edden, raee2@jhu.edu.

Ethical approval Ethics approval was obtained from the Ethics Committee of our Institution.

Consent to participate Informed consent (including informed parental consent) was obtained from all individual participants included in the study.

Consent to publish Additional informed consent (including informed parental consent) was obtained from all individual participants for whom identifying information is included in this article.

Conflict of interest The authors have no relevant financial or non-financial interests to disclose.

[13]Division of Neuroradiology, Park 367G, The Johns Hopkins University School of Medicine, 600 N. Wolfe St. B-112 D, Baltimore, MD 21287, USA

[14]Wendy Klag Center for Autism and Developmental Disabilities, Johns Hopkins University, Baltimore, USA

[15]Department of Mental Health, Bloomberg School of Public Health, Johns Hopkins University, Baltimore, USA

[16]Department of Pediatrics, Division of Neonatology and Newborn Nursery, University of WI–Madison, School of Medicine and Public Health, Madison, WI 53705, USA

[17]Department of Medical Physics, University of WI–Madison, School of Medicine and Public Health, Madison, WI 53705, USA

[18]Department of Medicine, Division of Newborn Medicine, Boston Children's Hospital, Harvard Medical School, Boston, MA, USA

[19]Children's Hospital Los Angeles, Los Angeles, CA 90027, USA

[20]Department of Radiology and Fetal and Neonatal Institute, CHLA Division of Neonatology, Department of Pediatrics, Children's Hospital of Los Angeles, University of Southern California, Los Angeles, CA 90033, USA

Abstract

J-difference-edited spectroscopy is a valuable approach for the detection of low-concentration metabolites with magnetic resonance spectroscopy (MRS). Currently, few edited MRS studies are performed in neonates due to suboptimal signal-to-noise ratio, relatively long acquisition times, and vulnerability to motion artifacts. Nonetheless, the technique presents an exciting opportunity in pediatric imaging research to study rapid maturational changes of neurotransmitter systems and other metabolic systems in early postnatal life. Studying these metabolic processes is vital to understanding the widespread and rapid structural and functional changes that occur in the first years of life. The overarching goal of this review is to provide an introduction to edited MRS for neonates, including the current state-of-the-art in editing methods and editable metabolites, as well as to review the current literature applying edited MRS to the neonatal brain. Existing challenges and future opportunities, including the lack of age-specific reference data, are also discussed.

Keywords

Edited MRS; Neonatal brain; J-difference editing; Low-concentration metabolites; Relaxation time

Introduction

Throughout early childhood, the brain undergoes a wide range of developmental processes that define the emerging central nervous system [1]. The developing brain is significantly different from the adult brain, metabolically [2, 3], structurally [4, 5], and functionally [6, 7]. Investigation of the immature brain is necessary to elucidate the course of biological and cognitive development and potentially offers new insight on the pathophysiology of neurodevelopmental and psychiatric disorders which begin to manifest during childhood

[8–10]. Perinatal brain injury and developmental brain abnormalities lead to lifelong neurological dysfunction which results in a substantial public health burden [11]. The high degree of plasticity in the developing brain supports the potential benefit of early intervention in these disorders [12]; however, due to a lack of mechanistic insight, the optimal timing and type of interventions is still not clear. Advances in pediatric magnetic resonance imaging (MRI) have allowed noninvasive studies of the developing anatomy [13, 14] and function [15], while in vivo magnetic resonance spectroscopy (MRS) provides complementary neurochemistry information in the developing brain [16, 17].

In contrast to other metabolic imaging techniques such as position emission tomography (PET), MRS does not involve ionizing radiation and can acquire metabolic information during a routine structural MRI exam by directly detecting signals from endogenous metabolites. Proton MRS (^{1}H-MRS) is widely used for noninvasive in vivo studies of brain metabolism. In developmental disorders [18–21], it can provide diagnostic information that is unique compared to the insight obtained from other MRI modalities and can also allow noninvasive monitoring of response to treatment [22]. Clinical pediatric MRS focuses on the strongest signals detectable from the more abundant metabolites, including but not limited to N-acetyl aspartate (NAA), creatine-containing compounds (Cr), choline-containing compounds (Cho), myo-inositol (mI), glutamine (Gln) and glutamate (Glu) (collectively as Glx), and, where it accumulates to detectable levels, lactate (Lac). Recent methodological advances have powered renewed interest in a number of less abundant but biologically important metabolites: γ-aminobutyric acid (GABA), N-acetyl aspartyl glutamate (NAAG), glutathione (GSH), ascorbate (Asc), aspartate (Asp), and Lac [23]. These metabolites are key biomarkers of neurotransmitter dysfunction [24, 25] and oxidative stress [26, 27], vital processes relevant across a range of neurodevelopmental and neuropsychiatric disorders. Detection of these less concentrated metabolites, whose MRS signals are smaller and highly overlapped, is most precisely achieved by J-difference editing [28, 29] and remains challenging when using conventional single-voxel MRS. J-difference editing (either Mescher-Garwood (MEGA) [30] or band selective inversion with gradient dephasing (BASING) [31]) is easily incorporated into the common Point RESolved Spectroscopy (PRESS) sequence and has been widely utilized in cognitive and clinical neuroscience research in adults [8–10, 32–35].

Despite increasing popularity in the adult population, J-difference editing has still not had a substantial impact in neonatal MRS, due to limited access to acquisition and analysis methodology, long acquisition times, and vulnerability to motion artifacts. Therefore, developing an appropriate protocol for pediatric edited MRS is of great importance. The purpose of this review is fourfold: (1) to discuss the metabolites that can be studied with edited MRS; (2) to present the methods of edited MRS for the non-expert reader; (3) to review those studies that have applied J-difference editing MRS in the neonatal brain; and (4) to describe the potential promise of neonatal edited MRS and current roadblocks to greater use.

Metabolite targets of edited MRS

The in vivo MR spectrum contains signals from metabolites with a range of concentrations. Here, we provide an overview of several low-concentration metabolites of particular biochemical interest in the developing brain, which can be measured by edited MRS. Table 1 summarizes the approximate in vivo metabolite concentrations in adults and neonates.

GABA is the main inhibitory neurotransmitter in the mature mammalian central nervous system (CNS) [46]. Its hyperpolarizing, inhibitory effect is mediated by three types of GABA receptors: $GABA_A$ (ligand-gated chloride ionotropic receptors), $GABA_B$ (G-protein-coupled receptors), and $GABA_C$ (ligand-gated chloride ionotropic receptors, with higher sensitivity and smaller currents following activation by GABA than $GABA_A$ receptors [47]). GABA-mediated inhibition is one-half of the crucial excitation-inhibition balance required for healthy brain function. Interestingly, GABA initially acts as the primary *excitatory* neurotransmitter during early brain development, and GABAergic transmission emerges earlier in neurodevelopment than glutamatergic excitatory transmission [48]. The switch from excitation to inhibition occurs at the first postnatal week [49], with the maturation of the membrane Cl^- gradient [50], as determined by cation-chloride cotransporters NKCC1 (Na^+-K^+-Cl^-Cl^-) and KCC2 (K^+-Cl^-) [46]. GABA neurotransmission is involved in many aspects of brain development and brain function, including synaptogenesis and synapse stabilization [51], learning [10, 52], and synaptic plasticity [53–55]. Previous studies in animals [56] and human pediatric populations [57–59] have demonstrated that GABA levels increase with age in the developing brain, which is not linear (much more rapid in the neonatal period)—concentrations double in the neonatal period [39] over 10 weeks—and then only approximate double over 10 years through childhood [58]. Dysfunction in GABAergic regulation (resulting from the insufficient production and/or increased utilization and break-down of GABA) has been implicated in various neurodevelopmental disorders, including autism spectrum disorder (ASD) [8, 9, 60].

Glutathione and ascorbate (Asc, also known as vitamin C) are the two most abundant antioxidants in the CNS [61]. They mitigate oxidative stress by donating electrons to various enzymatic and non-enzymatic reactions, thereby neutralizing the reactive oxygen species that are by-products of metabolism [62]. In brain tissue, they have different compartmentalization: GSH predominates in glia, whereas Asc predominates in neurons [61]. In the first day after birth in rats, cortical levels of Asc are high, as the neuronal population is far larger than the immature glial population [63]. As cortex develops, including gliogenesis, cortical Asc levels gradually fall and GSH levels increase [64]. In accordance with this, levels of Asc are higher in fetal and neonatal brains than in the adult human brain [65]. However, the temporal trajectory of brain GSH levels is less clear and may differ as a function of species, gender, and region [66]: studies of GSH have either shown decreased GSH levels [64], increased levels [61, 67], or no change [68, 69] with maturation. In humans, GSH levels have been shown to decline after birth (or trends for a reduction with age in the first year of postnatal development) [60]. The decrease in GSH and increase in Asc might be associated with the switch from neuron proliferation to differentiation during this period. Antioxidant deficiency, leading to poorly maintained redox homeostasis and oxidative stress, is a particular concern in the neonatal brain [70] and may

be implicated as contributory factors in the pathophysiology of ASD [27] and schizophrenia [71].

Lactate is one of the major energy sources for the brain [72, 73]. It is synthesized from pyruvate, the major glycolytic product, by the enzyme lactate dehydrogenase [74] under anaerobic conditions. Its level depends on age [75], cell type [74], and physiological/pathological conditions [76]. The brain has two major cell types, neurons and astrocytes. Astrocytes produce Lac. The extent to which neurons produce Lac by glycogenesis (especially in view of their lack of the 6-phosphofructo-2-kinase PFKFB3) is debated. It is likely that neurons *can* produce Lac (using alternative mechanisms for the regulation of glycolysis [77]), but also import Lac produced by astrocytes [78, 79]. Lactate acts as an important substrate for the developing brain [80]. For example, oligodendrocytes use Lac as a source of energy and lipid precursor during myelination [81]. It also acts as a signaling molecule, which is necessary for memory consolidation in learning tasks in animals [82–84], regulation in the GABAergic system [85], neuronal plasticity [86, 87], and neuronal excitability [88]. Previous work has shown neonates to have higher Lac levels in several brain regions [75], which subsequently decreases with increasing neuronal maturity [89] and decreasing transport across the blood–brain barrier [90]. The pathological imbalance between Lac clearance and generation can lead to accumulation of Lac, in turn, resulting in cellular damage and dysfunction [91]. Likewise, Lac rises acutely after hypoxic-ischemic brain injury and is a reliable early biomarker [92] and prognostic indicator after neonatal hypoxic-ischemic encephalopathy [93] and pediatric cardiac arrest [94]. Of note, the Lac doublet at 1.3 ppm should not be confused with propylene glycol (a solvent present in anti-seizure and other medications) at 1.1 ppm or alanine at 1.5 ppm, both of which are doublet peaks that invert at TE ~ 144 ms [95, 96].

NAAG is the most abundant neuropeptide and the third most abundant neurotransmitter in the human CNS [97]. NAAG has a higher concentration in white matter than gray matter [45], As a peptide formed from NAA and Glu [98], NAAG modulates levels of both, as well as having activity as a neurotransmitter/neuromodulator in its own right. NAAG also acts to regulate GABA [99] and dopamine [100] release. In rats, NAAG levels increase after birth, reaching maximum concentration approximately between postnatal 7–14 days, and then decreases with maturity [101, 102], In human infants, brain NAAG levels increase with age [1, 103], NAAG is generally understudied by MRS, in part due to the methodological challenge of resolving it from its constituents NAA and Glu [36]. However, MR spectra in the pediatric brain have substantially narrower linewidth (e.g., full width half maximum (FWHM) of the NAA acetyl singlet) than adult spectra (as discussed below), making sufficient resolution of the acetyl singlets of NAA and NAAG at 2.0 ppm more easily achievable.

Aspartate is a non-essential amino acid, synthesized by transamination of oxaloacetate (OAA). L-Asp is the more abundant isomer in the mammalian brain, required for protein assembly as well as being a precursor to other amino-acids: methionine, threonine, isoleucine, and lysine. However, D-Asp is more abundant than L-Asp in the developing brain [104, 105] and can modulate glutamatergic neurotransmission and neuroendocrine function [106, 107]. In preclinical models, levels of Asp appear to be higher early in

development and then decrease with time [56, 108]. However, in the human brain (as indicated by postmortem samples of the putamen), Asp levels increase steeply within the first postnatal year and remain fairly constant throughout life [109]. The dysregulation of Asp metabolism and signaling in the brain impacts the pathophysiology of psychiatric disorders, such as schizophrenia [110, 111] and ASD [110].

There is a dynamic equilibrium in the brain among these metabolites, and the level of each (which is what MRS detects) reflects the balance of formation and catabolism. Changes in the level of one compound can have far-reaching effects on the reaction kinetics of the metabolic pathways that connect them. For example, in the brains of individuals with chronic alcoholism, down-regulated cystine/Glu exchange leads to decreased levels of cysteine (Cys), which in turn rate limit the production of glutathione, as well as increased excitatory activity due to higher synaptic Glu levels [112]. In general, as the metabolite with the highest concentration in the brain, Glu takes a central role in the biochemistry of many MRS-visible metabolites, as seen in Fig. 1. In both astrocytes and neurons, Glu is synthesized from the tricarboxylic acid cycle (TCA-cycle)-intermediate α-ketoglutarate [113]. Synaptic Glu released from neurons is largely taken up by astrocytes, where it is converted to glutamine (Gln, also MRS-visible) and transported back to be taken up by neurons and deaminated to reform Glu. GABA is also synthesized from Glu, and in addition to acting as a neurotransmitter, GABA can be transferred to succinic semialdehyde (SSA) (then succinate) and recycled into the TCA cycle [114, 115]. Glutathione is a tripeptide of Glu with Cys and glycine, which undergoes an oxidative dimerization to glutathione sidulfide (GSSG); both engage in free radical neutralization cascades with ascorbate to maintain cellular redox balance [116]. Acetyl-CoA is a second key hub compound, which has relatively low concentration and very high flux, replenishing the TCA cycle with new carbon elements. Acetyl-CoA is also used to synthesize NAA by acetylating aspartate (which is itself formed from the TCA-cycle intermediate OAA). NAAG is further synthesized from NAA and Glu and therefore indirectly modulates their levels.

Methodological summary of advanced MRS

Proton MRS (^{1}H-MRS) is a noninvasive methodology for in vivo detection of endogenous metabolites in clinical [93] and basic neuroscience research [23]. The in vivo spectrum is a relaxation-weighted sum of all the proton signals that can be excited from a region of tissue. As shown in Fig. 2, the pediatric spectrum differs from the adult spectrum in two important ways. Firstly, the concentration of several prominent signals (e.g., NAA) is different at various stages of development (neonate, pediatrics, adult), reflecting maturation and reorganization. Secondly, the linewidth of signals in the pediatric brain is narrower, due to reduced myelination [117] and metal deposits[118], resulting in higher SNR and reduced spectral overlap.

Scalar coupling in MRS

One feature of MRS that is not commonly considered in MRI is the scalar (or *J*-) coupling. This is a mechanism by which hydrogen nuclei that are attached to adjacent carbons within a molecule can exchange information, determining the appearance (specifically the

multiplicity) of signals in the MR spectrum. As an example, the molecular structure and MR spectrum of lactate are shown in Fig. 3A. The methyl signal at 1.3 ppm has a doublet character because the resonance frequency of the methyl spins is influenced by the spin-state (i.e., spin-up or spin-down, alpha or beta state) of the methine proton. If that adjacent spin is spin-up, as is the case in 50% of molecules, the resonant frequency is increased; if that adjacent spin is spin-down, as in the remaining 50%, the resonant frequency is decreased. This results in a splitting of the methyl signal into a 1:1 doublet. The signal from the methine proton is split into a 1:3:3:1 quartet because the spin-states of the methyl protons collectively are either: all spin-up (in 1/8 of molecules); two spin-up and one spin-down (in 3/8); one spin-up and two spin-down (in 3/8); or all spin-down (in 1/8). Thus, the appearance of each multiplet in a coupled spin system has a multiplicity of $n + 1$, where n is the number of adjacent protons. The GABA molecule, for example, as shown in Fig. 3B, has three mutually coupled methylene CH_2 groups. The terminal CH_2s, each of which is only coupled to two adjacent protons, give rise to triplet-like signals in the spectrum. The central CH_2 which has four adjacent protons gives a more complex quintet-like signal.

Scalar coupling splits the MR signals from many low-concentration metabolites into complex multiplets, such that the dispersion of signals along the chemical shift axis is limited compared with the width of signals [29]. Furthermore, the resonances of GABA, glutathione, NAAG, and other lower-concentration metabolites with coupled spin systems remain overlapped with resonances from other more concentrated metabolites. J-difference editing can solve this overlap problem, using a targeted acquisition strategy to isolate resonances from a particular metabolite of interest. Frequency-selective radiofrequency (RF) pulses can be used to modulate the evolution of coupled spin systems during the echo time; a spectrum containing only those signals impacted by the editing pulses can be obtained by subtracting subexperiments acquired with, and without, editing pulses [28]. These “editing” pulses directly manipulate the evolution of scalar coupling during the experiment, allowing coupled signals to be separated on the basis of where in the spectrum their coupling partners lie. This approach is most commonly combined with single-voxel localization in MEGA-PRESS (Mescher-Garwood Point Resolved Spectroscopy [30, 119]) or MEGA-sLASER (MEGA-semi-localization by adiabatic selective refocusing) [120, 121].

J-difference editing

J-difference editing of GABA and lactate is illustrated in Fig. 4. The GABA spectrum has signals at 1.9 ppm, 2.3 ppm, and 3.0 ppm; editing pulses are applied to the 1.9-ppm multiplet to modulate evolution of the 3-ppm multiplet and change the form of the signal as seen in panel A. Subtraction of “ON” and “OFF” subspectra acquired with and without editing pulses removes the large 3-ppm Cr signal (and any other signals that were not affected by the editing pulses) to reveal an edited GABA signal at 3 ppm (panel B). GABA signals are typically edited at a TE of ~ 68 ms, since this is the TE at which the outer peaks of the 3-ppm signal are inverted in the OFF spectrum. Similarly, the Lac spectrum (panel C) has signals at 1.3 ppm from the methyl (CH_3) protons and at 4.1 ppm from the methine (CH) protons [122]. Edited detection of the methyl resonance can be achieved by applying editing pulses at 4.1 ppm [123]. At a TE of 140 ms, the methyl resonance is inverted in the “off” subspectrum and refocused in the “on” subspectrum (panel C). The appropriate

TE for optimal editing depends on the coupled spin systems that are being targeted; TEs from 68 to 140 ms are optimal for different metabolites. The optimal TE is determined by the multiplicity of the signal to be edited. To edit the triplet-like GABA signal at 3 ppm, in which the outer peaks are separated by ~ 14 Hz, a TE of ~ 68 ms is appropriate. Similarly, to edit the Lac doublet at 1.3 ppm, which has a ~ 14 Hz splitting, a TE of ~ 140 ms is appropriate. The duration of the scan for each GABA and Lac spectrum is 10 min 40 s for 320 averages with TR = 2 s. In both cases, the resolution afforded by editing is not absolute: the GABA-edited spectrum also contains contributions from related metabolites such as homocarnosine [124] and macromolecular signals (often labeled GABA+); lactate-edited spectra also contain signals from beta-hydroxybutyrate (BHB) [125] and macromolecular signals at 1.2 and 1.4 ppm [126].

Advanced editing

J-difference-edited experiments usually proceed at a rate of one region-of-interest and one metabolite-of-interest per experiment. Double editing with (DEW) MEGA-PRESS allows two MEGA-PRESS experiments to be carried out simultaneously, provided that the four relevant signals (the two target signals to which editing pulses are applied, and the two detected signals) can be resolved from one another [127]. DEW has been applied to measurements of glutathione and ascorbate, as an antioxidant profile [127], and GSH and lactate [128].

Hadamard-encoded editing allows simultaneous editing of two or more signals and only requires frequency separation of the editing target signals. HERMES (Hadamard Encoding and Reconstruction of MEGA-edited Spectroscopy) uses a four- (or more-) step editing scheme that amounts to performing more than one MEGA-PRESS experiment at the same time. This editing scheme ensures that the different target signals are treated independently and different edited spectra can be extracted from the dataset by different Hadamard combinations. HERMES has been used to separate the aspartate signals of NAA, NAAG and Asp [129, 130], GABA and glutathione [131, 132], and GABA, GSH, and ethanol [133]. HERCULES (Hadamard Editing Resolves Chemicals Using Linear-combination Estimation of Spectra) (Fig. 5) can separate up to eight edited metabolites [134], using a combination of multi-step editing schemes and multi-spectrum linear combination modeling. These advanced acquisition schemes address a key limitation of edited MRS, the need for a longer scan time to obtain resolved resonances from several metabolites within a single MR exam. Despite the potential drawback of sensitivity to motion and instabilities, their development paves the way towards a more widespread application of edited MRS in the clinical environment. Table 2 lists available MRS methods and summarizes the major advantages and disadvantages.

Single-voxel vs. MRSI

The most common sequence for edited MRS, MEGA-PRESS [30], adds frequency-selective editing pulses to a single-voxel PRESS localization sequence [119]. Magnetic resonance spectroscopic imaging (MRSI) combines spatial encoding gradients with a spectroscopic read-out in order to acquire data in multiple brain regions simultaneously and yield spatial maps of metabolite levels [23]. Given the challenges of accurate subtraction (see discussion

of subtraction artifacts in [139–141]), single-voxel methods benefit from post-processing frequency and phase alignment, which is not typically possible for MRSI. Thus, the "MRSI vs. single-voxel" comparison largely weighs "more data" against "greater robustness to motion." This, as well as long acquisition times and complex processing, limits the clinical application of MRSI, particularly in pediatric populations [138].

Field strength

Currently, MRS is largely performed at three main field strengths: 1.5 T, 3 T, and 7 T. Clinically, 1.5 T has been the "workhorse" field strength, but 3 T is increasingly being used, particularly in academic medical centers with MR research programs. In research, 3 T is the "workhorse" field strength, and 7 T is an emerging discipline. For MRS, the field strength has two main impacts: the primary motivation for higher field strength, increased SNR; and a secondary benefit that multiplet splittings, which remain constant in terms of Hz, are increasingly spread along the ppm axis, leading to improved resolution of signals. In edited MRS, there are two additional impacts with increasing field strength: the rate of T_2 relaxation increases (mitigating some of the SNR gains for edited experiments acquired at medium/long TE) and the effective selectivity (in ppm) of editing pulses increases. Thus, the duration of an editing pulse with the same degree of selectivity scales inversely with field strength. This, combined with optimal editing TEs (as discussed above), limits the effectiveness of GABA editing at 1.5 T. Improved selectivity of editing that comes with higher field strengths is desirable for specificity but also reduces the robustness of experiments to scanner instability and patient motion (a particular concern for neonatal MRS).

Applications of edited MRS in neonates

Literature review methods

Primary search terms applied to PubMed on June 23, 2021, were "edited MRS neonates" (7 results), "edited MRS baby brain" (3 results), and "edited MRS newborn brain" (5 results). Additional searches were made based on known methods (such as "GABA MRS neonates" (27 results), "GSH MRS neonates" (3 results), "Lactate MRS neonates" (134 results)) and known authors (such as "Kreis, MRS, neonates" (4 results), "Cady, MRS, neonates" (15 results), "Basu, MRS, neonates" (4 results) choice based on the prior search results). These search results were filtered to remove the following: (1) all references that do not use edited MRS; (2) all studies of non-human subjects; (3) all studies not carried out in vivo; (4) all studies of organs other than the brain; and (5) all studies of adult subjects. Table 3 shows an overview of published edited MRS studies in the neonatal brains.

Lactate-edited MRS

The first publication of edited MRS in the neonatal brain [135] applied lactate-edited 3D MRSI [142] to assess the effect of pentobarbital sedation in metabolites of healthy preterm infants. This study showed that Lac level in the basal ganglia (BG) was significantly lower in the fourteen neonates with pentobarbital sedation compared to the twenty-nine neonates scanned without sedation. Given that other metabolite ratios did not differ between groups, the authors suggested that pentobarbital-related down-regulation of glycolysis accounted for

the results. The acquisition protocol imaged an 8 × 8 × 8 array of 1 cm^3 voxel, lasting 18 min. A review of neonatal MRS from the same group also showed three Lac-edited example spectra [17]. These spectra establish the feasibility of the method and illustrate Lac levels increasing with the severity of the hypoxic injury.

A later conference abstract [136] applied the BASING technique to determine lactate levels in the neonatal brain and to illustrate the benefits of editing for improved visualization and quantification of the Lac resonance. The Lac doublet at 1.3 ppm was masked by strong lipid signals in unedited short-TE (35 ms) spectra, and absent from unedited long-TE (144 ms) spectra, likely due to spatial heterogeneity in coupling evolution [143]. Despite the benefits of editing, most clinical MRS in neonates has applied unedited methods to quantify Lac, often with TEs of 144 ms [144] or 288 ms [76]. While elevated Lac is a hallmark of perinatal hypoxia, Lac is present at quantifiable levels in healthy neonates [135], with levels decreasing into infancy and childhood [75].

GABA-edited MRS

A majority of studies applying edited MRS in the neonatal brain have used the MEGA-PRESS sequence to detect GABA. In a study examining GABA levels and resting-state functional connectivity associated with preterm birth, Kwon et al. [137] observed lower GABA levels in preterm infants than term infants (scanned at mean median postmenstrual age (PMA) 42.6w and 42.5w, respectively). The cohort was recruited from 2010 to 2013 making this the earliest example of GABA-edited MRS in neonates and included 18 preterm and 21 term neonates. The study focused on a 2 × 3 × 3 cm^3 region in the right frontal lobe, acquiring up to 20 min of data per subject in a protocol with 8 acquisition blocks (TR = 1.5 s). Relationships between GABA levels and resting-state functional connectivity were also notably different in the two groups.

Tanifuji et al. [40] reported the first longitudinal study of GABA levels in twenty preterm infants (median postmenstrual age (PMA) at birth 30 weeks), acquiring data at two time points: 37–46 postmenstrual weeks and 64–73 postmenstrual weeks. Although significant increases in NAA, Glu-Gln, and Cr and decreases in mI were observed, there was no significant change in GABA between the time points. The study acquired 7 min of data from a 2.5 × 2.5 × 2.5 cm^3 voxel in the right BG.

Tomiyasu et al. [57] reported lower levels of GABA in neonates than children, continuing the theme of increasing GABA levels through early development. The study compared GABA levels in cerebellar and BG regions, in 38 neonates (preterm: 23–36w, studied at a PMA of 35–41w; term: 37–41w, studied at a PMA of 38–43w) and 12 school-age children (mean 10.2 years; range 6–16 years). Data were acquired for 3 min per voxel, with voxels ranging from 4 to 9 cm^3 in infants and 13 to 37 cm^3 in children. This study raises the concern of appropriate signal quantification, especially in the context of changing levels and relaxation rates of the potential reference signals across development.

Basu et al. [39] also assessed GABA levels in a larger cohort of preterm infants. A negative correlation was seen between GABA levels with gestational age (GA), while a positive correlation was seen with postnatal age. Among the preterm infants, those born before

28 weeks were shown to have significantly higher GABA levels at TEA than those born after. GABA levels were also higher in male infants, compared to females; groups were well-matched in GA at birth and birth weight. The study focused on a 2.0 × 1.5 × 1.5 cm^3 voxel in the right frontal lobe, acquiring data for 8 min.

Most recently, Yanez Lopez et al. [41] applied HERMES to simultaneously edit GABA and glutathione in 18 healthy neonates, scanned between 39 and 47 weeks PMA. Measurements were made in regions of the anterior cingulate cortex (3.1 × 2.5 × 2.0 cm^3) and left thalamus (2.5 × 2.5 × 2.5 cm^3), acquiring data for 10 min. Regional differences were observed in GABA+ and Glu levels, but not GSH levels. The manuscript focuses substantially on methodological considerations, including the importance of incorporating tissue segmentation and correction and optimized fitting for GABA+ quantification.

Acquisition time and voxel size

As mentioned above and summarized in Table 3, edited data have been acquired at a broad range of SNR levels, as can be inferred from the acquisition time and voxel size. At the lower end, Tomiyasu et al. made GABA + measurements down to 3.7 cm^3 voxels acquired for 3 min. Comparing to a common benchmark for adult studies of 27 cm^3 acquired for 10 min [140], this acquisition has over 90% lower SNR. Infant brains are smaller than adult brains, forcing authors to choose between diminished anatomical specificity and reduced SNR. Further consideration of the challenges of neonatal MRS is given below.

Quantification and tissue correction

Quantification of MRS signals relies upon an internal reference signal, most commonly the Cr singlet or the unsuppressed water signal (either with or without relaxation correction). However, it should be noted that Cr levels change dramatically during the first 2 years of life, making this a poor reference, in particular, in studies on early development [1]. Of the seven studies included in Table 3, the majority report both water-referenced and Cr-referenced levels of the edited metabolite signals. The degree of tissue and relaxation correction applied in water-referenced studies varies, as it does in the adult literature. Tissue correction is very important, especially given uncertainties about voxel composition due to the partial volume effect.

Influence of sedation

Clinical imaging of neonates is occasionally performed under sedation. Research studies have so far been reported both using sedated and non-sedated subjects, but the effect of sedation on edited metabolite signals has not been systematically characterized.

Challenges and opportunities for neonatal J-edited MRS

J-difference-edited MRS is the recommended approach [145] for detecting low-concentration metabolites with overlapped spectra in the adult brain. However, in order to advance the application of this technique in pediatrics, several challenges must be addressed, starting with SNR. At birth, the newborn brain is about 1/4 the volume of a mature adult. Although it is possible to scale voxel size to approximately 1/4 that of an adult, SNR

scales directly with volume, so this approach would reduce SNR by approximately 75%. Furthermore, while this can theoretically be counteracted by increasing the number of signal averages (NSA), a 16-fold increase in scan time is not practical.

Notably, the infant brain does offer several distinct advantages, which collectively mitigate some of these challenges, enhancing SNR as well as chemical resolution. First, transverse relaxation is substantially longer in infants, which increases SNR and results in narrower linewidth. Second, as noted earlier, the newborn brain has very little iron and a low myelin content, leading to better B_0 homogeneity and again narrower linewidth. Both of these are favorable for editing and underscore the need for optimized sequences for infants that capitalize on these advantages.

A second key challenge is motion, which is particularly important for motion-sensitive methods like edited MRS [139]. Infants and young children move, and, even when imaged during natural sleep or with extensive training prior to scanning [146], may display occasionally twitches let alone awaken (or abort) in the middle of (long) sequences. Thus, the availability of prospective motion correction, as has been developed and now increasingly used in structural imaging [147], would greatly enhance the feasibility and rigor of edited MRS in pediatric populations. Excitingly, these techniques have been applied to single-voxel MRS and MRSI [133, 148] though not yet widely available as product sequences or works-in-progress (WIPs).

Thirdly, even in the event that high-quality data can be acquired in the pediatric brain, there is an important lack of age-appropriate reference data, e.g., metabolite relaxation times, MR-visible tissue water content, and macromolecular background spectra. The consensus for MRS quantification within the MRS research community is that these correction factors are required for modeling and quantification [149], and adult reference values are not appropriate. As one example of the limited reference data, Table 4 summarizes the prior literature [76, 150–153] on neonatal metabolite relaxation times, acquired with a range of techniques, field strengths, brain regions, etc., and highlights its limited scope. Due to significant tissue water content changes that occur during early brain development [154], the longitudinal relaxation times (T_1) undergo rapid maturation [155] and differ substantially between children and adults (and even between children). Similarly, due to an increase in myelination [156], reduction of free water content, and increased white-matter volume, transverse relaxation times (T_2) also substantially change during development [155]. The scarcity of reports indicates that one important future effort will be to establish age-dependent models for each of the necessary correction factors and/or to develop advanced measurement techniques that include relaxometry without increasing acquisition times [157, 158].

As we consider future applications, it is important to recognize that 1 in 54 children in the USA will be diagnosed with ASD [159], 1 in 150 with epilepsy [160], and 1 in 10 with attention deficit hyperactivity disorder (ADHD) [161]. These and many other disorders are thought to have their genesis in infancy, with small molecules such as glutamine and GABA playing a central role. In addition, numerous therapeutic trials of neonatal neuroprotectants are underway (HELIX (Hypothermia for Encephalopathy in Low- and

Middle-Income Countries), High-Dose Erythropoietin for Asphyxia and Encephalopathy (HEAL), Erythropoietin and Darbepoetin in Neonatal Encephalopathy Trial (EDEN) and Erythropoietin Monotherapy for Brain Regeneration After Neonatal Encephalopathy in Low- and Middle-Income Countries (EMBRACE)) [162–164], where changes in small molecules have the potential to inform dosing decisions and individual treatment response. Thus, the widespread availability of reliable and accurate methods for edited MRS in the neonatal population could have a major impact in neonatal disorders and pave the way for personalized approaches to early diagnosis and management. Furthermore, utilizing edited MRS methodologies within the design of large-scale neurodevelopmental studies, such as the recently announced Healthy Brain and Cognitive Development (HBCD) study [165, 166], would allow characterization of normal trajectories and improve our understanding of the complex interactions between genes and environment on the biochemical aspects of brain development from birth through the first decade of life.

Conclusion

Edited MRS is a powerful and valuable methodology to detect low-concentration metabolites reflecting various critical physiological processes, such as neurotransmitters GABA and Glu, antioxidants glutathione and ascorbate, and the product of anaerobic glycolysis lactate. Edited MRS offers considerable potential to augment pediatric MRI for detecting low-concentration metabolites related to developmental abnormalities. To enhance the feasibility and rigor of this approach in pediatrics and, ultimately, its utility to inform neurodevelopment, there needs to be investment from the MRS community ideally in partnership with pediatric neuroradiologists and developmental neuroscientists, leading to new optimized sequences with prospective motion correction and the availability of age-appropriate reference data.

Funding

This work is supported by National Institutes of Health (NIH) grants R01 EB016089; R01 EB023963; R21 HD100869; P41 EB031771; R00 AG062230; 1R34DA050292-01; K23 HD099309.

This work is also funded in part through a project grant awarded by Action Medical Research [GN 2728], a Medical Research Council (MRC) transition support fellowship [MR/V 036,874/1], and the Wellcome Engineering and Physical Sciences Research Council (EPSRC) Centre for Medical Engineering at Kings College London [WT 203,148/Z/16/Z].

References

1. Bluml S et al. (2013) Metabolic maturation of the human brain from birth through adolescence: insights from in vivo magnetic resonance spectroscopy. Cereb Cortex 23:2944–2955 [PubMed: 22952278]
2. Pouwels PJ et al. (1999) Regional age dependence of human brain metabolites from infancy to adulthood as detected by quantitative localized proton MRS. Pediatr Res 46:474–485 [PubMed: 10509371]
3. Kreis R et al. (2002) Brain metabolite composition during early human brain development as measured by quantitative in vivo 1H magnetic resonance spectroscopy. Magn Reson Med 48:949–958 [PubMed: 12465103]
4. Zhang L et al. (2005) MR quantitation of volume and diffusion changes in the developing brain. AJNR Am J Neuroradiol 26:45–49 [PubMed: 15661698]

5. Durston S et al. (2001) Anatomical MRI of the developing human brain: what have we learned? J Am Acad Child Adolesc Psychiatry 40:1012–1020 [PubMed: 11556624]
6. Lin W et al. (2008) Functional connectivity MR imaging reveals cortical functional connectivity in the developing brain. AJNR Am J Neuroradiol 29:1883–1889 [PubMed: 18784212]
7. Houde O et al. (2010) Mapping numerical processing, reading, and executive functions in the developing brain: an fMRI meta-analysis of 52 studies including 842 children. Dev Sci 13:876–885 [PubMed: 20977558]
8. Harris AD et al. (2021) Relationship between GABA levels and task-dependent cortical excitability in children with attention-deficit/hyperactivity disorder. Clin Neurophysiol 132:1163–1172 [PubMed: 33780723]
9. Puts NAJ et al. (2017) Reduced GABA and altered somatosensory function in children with autism spectrum disorder. Autism Res 10:608–619 [PubMed: 27611990]
10. Kolasinski J et al. (2019) The dynamics of cortical GABA in human motor learning. J Physiol 597:271–282 [PubMed: 30300446]
11. Szpir M (2006) New thinking on neurodevelopment. Environ Health Perspect 114:A100–A107 [PubMed: 16451834]
12. Ismail FY, Fatemi A, Johnston MV (2017) Cerebral plasticity: windows of opportunity in the developing brain. Eur J Paediatr Neurol 21:23–48 [PubMed: 27567276]
13. Giedd JN, Rapoport JL (2010) Structural MRI of pediatric brain development: what have we learned and where are we going? Neuron 67:728–734 [PubMed: 20826305]
14. Thayyil S et al. (2013) Post-mortem MRI versus conventional autopsy in fetuses and children: a prospective validation study. Lancet 382:223–233 [PubMed: 23683720]
15. Freilich ER, Gaillard WD (2010) Utility of functional MRI in pediatric neurology. Curr Neurol Neurosci Rep 10:40–46 [PubMed: 20425225]
16. Vigneron DB et al. (2001) Three-dimensional proton MR spectroscopic imaging of premature and term neonates. AJNR Am J Neuroradiol 22:1424–1433 [PubMed: 11498441]
17. Xu D, Vigneron D (2010) Magnetic resonance spectroscopy imaging of the newborn brain–a technical review. Semin Perinatal 34:20–27
18. Kacinski M et al. (2006) Preliminary assessment of HMRS clinical usefulness in children with partial epilepsy. Przegl Lek 63:1191–1197 [PubMed: 17348414]
19. Filippi CG et al. (2002) Developmental delay in children: assessment with proton MR spectroscopy. AJNR Am J Neuroradiol 23:882–888 [PubMed: 12006297]
20. Smigielska-Kuzia J et al. (2010) Amino acid metabolic processes in the temporal lobes assessed by proton magnetic resonance spectroscopy (1H MRS) in children with Down syndrome. Pharmacol Rep 62:1070–1077 [PubMed: 21273664]
21. Sato T et al. (2014) Neonatal case of classic maple syrup urine disease: usefulness of (1) H-MRS in early diagnosis. Pediatr Int 56:112–115 [PubMed: 24548198]
22. Zarifi M, Tzika AA (2016) Proton MRS imaging in pediatric brain tumors. Pediatr Radiol 46:952–962 [PubMed: 27233788]
23. Zhu H, Barker PB (2011) MR spectroscopy and spectroscopic imaging of the brain. Methods Mol Biol 711:203–226 [PubMed: 21279603]
24. Ala-Korpela M et al. (1995) Quantification of metabolites from single-voxel in vivo 1H NMR data of normal human brain by means of time-domain data analysis. MAGMA 3:129–136 [PubMed: 8749730]
25. Wassef A, Baker J, Kochan LD (2003) GABA and schizophrenia: a review of basic science and clinical studies. J Clin Psychopharmacol 23:601–640 [PubMed: 14624191]
26. Sawa A, Sedlak TW (2016) Oxidative stress and inflammation in schizophrenia. Schizophr Res 176:1–2 [PubMed: 27395767]
27. Bjorklund G et al. (2020) Oxidative stress in autism spectrum disorder. Mol Neurobiol 57:2314–2332 [PubMed: 32026227]
28. Rothman DL et al. (1993) Localized 1H NMR measurements of gamma-aminobutyric acid in human brain in vivo. Proc Natl Acad Sci U S A 90:5662–5666 [PubMed: 8516315]

29. Harris AD, Saleh MG, Edden RA (2017) Edited (1) H magnetic resonance spectroscopy in vivo: Methods and metabolites. Magn Reson Med 77:1377–1389 [PubMed: 28150876]
30. Mescher M et al. (1998) Simultaneous in vivo spectral editing and water suppression. NMR Biomed 11:266–272 [PubMed: 9802468]
31. Star-Lack J et al. (1997) Improved water and lipid suppression for 3D PRESS CSI using RF band selective inversion with gradient dephasing (BASING). Magn Reson Med 38:311–321 [PubMed: 9256113]
32. Stagg CJ et al. (2011) Relationship between physiological measures of excitability and levels of glutamate and GABA in the human motor cortex. J Physiol 589:5845–5855 [PubMed: 22005678]
33. Chen CM et al. (2014) GABA level, gamma oscillation, and working memory performance in schizophrenia. Neuroimage Clin 4:531–539 [PubMed: 24749063]
34. Kegeles LS et al. (2012) Elevated prefrontal cortex gamma-aminobutyric acid and glutamate-glutamine levels in schizophrenia measured in vivo with proton magnetic resonance spectroscopy. Arch Gen Psychiatry 69:449–459 [PubMed: 22213769]
35. Gong T et al. (2018) Inhibitory motor dysfunction in Parkinson's disease subtypes. J Magn Reson Imaging 47:1610–1615 [PubMed: 28960581]
36. Govindaraju V, Young K, Maudsley AA (2000) Proton NMR chemical shifts and coupling constants for brain metabolites. NMR Biomed 13:129–153 [PubMed: 10861994]
37. Klunk WE et al. (1996) Quantitative 1H and 31P MRS of PCA extracts of postmortem Alzheimer's disease brain. Neurobiol Aging 17:349–357 [PubMed: 8725895]
38. Van Zijl PC, Barker PB (1997) Magnetic resonance spectroscopy and spectroscopic imaging for the study of brain metabolism. Ann N Y Acad Sci 820:75–96 [PubMed: 9237450]
39. Basu SK et al. (2020) Age and sex influences gamma-aminobutyric acid concentrations in the developing brain of very premature infants. Sci Rep 10:10549 [PubMed: 32601466]
40. Tanifuji S et al. (2017) Temporal brain metabolite changes in preterm infants with normal development. Brain Dev 39:196–202 [PubMed: 27838187]
41. Maria YL et al. (2021) Simultaneous quantification of GABA Glx and GSH in the neonatal human brain using magnetic resonance spectroscopy. Neuroimage 233:117930 [PubMed: 33711485]
42. Siegel GJ, Agranoff BW, Albers RW, Molinoff PB (1988) Basic neurochemistry: molecular, cellular, and medical aspects. Raven Press, New York
43. Terpstra M, Ugurbil K, Tkac I (2010) Noninvasive quantification of human brain ascorbate concentration using 1H NMR spectroscopy at 7 T. NMR Biomed 23:227–232 [PubMed: 19655342]
44. Terpstra M, Gruetter R (2004) 1H NMR detection of vitamin C in human brain in vivo. Magn Reson Med 51:225–229 [PubMed: 14755644]
45. Pouwels PJ, Frahm J (1997) Differential distribution of NAA and NAAG in human brain as determined by quantitative localized proton MRS. NMR Biomed 10:73–78 [PubMed: 9267864]
46. Li K, Xu E (2008) The role and the mechanism of gamma-aminobutyric acid during central nervous system development. Neurosci Bull 24:195–200 [PubMed: 18500393]
47. Enz R (2001) GABA(C) receptors: a molecular view. Biol Chem 382:1111–1122 [PubMed: 11592392]
48. Bak LK, Schousboe A, Waagepetersen HS (2006) The glutamate/GABA-glutamine cycle: aspects of transport, neurotransmitter homeostasis and ammonia transfer. J Neurochem 98:641–653 [PubMed: 16787421]
49. Valeeva G, Valiullina F, Khazipov R (2013) Excitatory actions of GABA in the intact neonatal rodent hippocampus in vitro. Front Cell Neurosci 7:20 [PubMed: 23467988]
50. Ben-Ari Y et al. (2012) The GABA excitatory/inhibitory shift in brain maturation and neurological disorders. Neuroscientist 18:467–486 [PubMed: 22547529]
51. Jelitai M, Madarasz E (2005) The role of GABA in the early neuronal development. Int Rev Neurobiol 71:27–62 [PubMed: 16512345]
52. Frangou P, Correia M, and Kourtzi Z (2018) GABA, not BOLD, reveals dissociable learning-dependent plasticity mechanisms in the human brain. Elife, 7.

53. Castro-Alamancos MA, Donoghue JP, Connors BW (1995) Different forms of synaptic plasticity in somatosensory and motor areas of the neocortex. J Neurosci 15:5324–5333 [PubMed: 7623155]
54. Trepel C, Racine RJ (2000) GABAergic modulation of neocortical long-term potentiation in the freely moving rat. Synapse 35:120–128 [PubMed: 10611637]
55. Lunghi C et al. (2015) Short-term monocular deprivation alters GABA in the adult human visual cortex. Curr Biol 25:1496–1501 [PubMed: 26004760]
56. Saransaari P, Oja SS (1998) Release of endogenous glutamate, aspartate, GABA, and taurine from hippocampal slices from adult and developing mice under cell-damaging conditions. Neurochem Res 23:563–570 [PubMed: 9566593]
57. Tomiyasu M, et al. (2017) In vivo estimation of gamma-aminobutyric acid levels in the neonatal brain. NMR Biomed, 30.
58. Saleh MG et al. (2020) Effect of age on GABA+ and glutathione in a pediatric sample. AJNR Am J Neuroradiol 41:1099–1104 [PubMed: 32381543]
59. Larsen RJ et al. (2021) Quantification of magnetic resonance spectroscopy data using a combined reference application in typically developing infants. NMR Biomed 34:e4520 [PubMed: 33913194]
60. Tong J et al. (2016) Do glutathione levels decline in aging human brain? Free Radic Biol Med 93:110–117 [PubMed: 26845616]
61. Rice ME, Russo-Menna I (1998) Differential compartmentalization of brain ascorbate and glutathione between neurons and glia. Neurosci 82:1213–1223
62. Pompella A et al. (2003) The changing faces of glutathione, a cellular protagonist. Biochem Pharmacol 66:1499–1503 [PubMed: 14555227]
63. Parnavelas JG et al. (1983) A qualitative and quantitative ultrastructural study of glial cells in the developing visual cortex of the rat. Philos Trans R Soc Lond B Biol Sci 301:55–84 [PubMed: 6135232]
64. Nanda D, Tolputt J, Collard KJ (1996) Changes in brain glutathione levels during postnatal development in the rat. Brain Res Dev Brain Res 94:238–241 [PubMed: 8836583]
65. Adlard BP, De Souza SW, Moon S (1974) Ascorbic acid in fetal human brain. Arch Dis Child 49:278–282 [PubMed: 4830116]
66. Moyse E et al. (2015) Gender- and region-dependent changes of redox biomarkers in the brain of successfully aging LOU/C rats. Mech Ageing Dev 149:19–30 [PubMed: 25956602]
67. Kudo H et al. (1990) Quantitative analysis of glutathione in rat central nervous system: comparison of GSH in infant brain with that in adult brain. Brain Res 511:326–328 [PubMed: 2334850]
68. Di Toro CG et al. (2007) Sensitivity of cerebellar glutathione system to neonatal ionizing radiation exposure. Neurotoxicology 28:555–561 [PubMed: 17267041]
69. Rahaman SO et al. (2001) Hypothyroidism in the developing rat brain is associated with marked oxidative stress and aberrant intraneuronal accumulation of neurofilaments. Neurosci Res 40:273–279 [PubMed: 11448519]
70. Ozsurekci Y, Aykac K (2016) Oxidative stress related diseases in newborns. Oxid Med Cell Longev 2016:2768365 [PubMed: 27403229]
71. Gorny M, et al. (2019) Glutathione deficiency and alterations in the sulfur amino acid homeostasis during early postnatal development as potential triggering factors for schizophrenia-like behavior in adult rats. Molecules, 24.
72. Wyss MT et al. (2011) In vivo evidence for lactate as a neuronal energy source. J Neurosci 31:7477–7485 [PubMed: 21593331]
73. Zilberter Y, Zilberter T, Bregestovski P (2010) Neuronal activity in vitro and the in vivo reality: the role of energy homeostasis. Trends Pharmacol Sci 31:394–401 [PubMed: 20633934]
74. Rae CD (2014) A guide to the metabolic pathways and function of metabolites observed in human brain 1H magnetic resonance spectra. Neurochem Res 39:1–36 [PubMed: 24258018]
75. Tomiyasu M et al. (2016) Normal lactate concentration range in the neonatal brain. Magn Reson Imaging 34:1269–1273 [PubMed: 27466138]
76. Lally PJ (2018) Magnetic resonance spectroscopy in hypoxic ischaemic encephalopathy. Published, Imperial College London

77. Berg JM TJ, Stryer L 2002. The glycolytic pathway is tightly controlled.
78. Brooks GA (2009) Cell-cell and intracellular lactate shuttles. J Physiol 587:5591–5600 [PubMed: 19805739]
79. Magistretti PJ, Allaman I (2018) Lactate in the brain: from metabolic end-product to signalling molecule. Nat Rev Neurosci 19:235–249 [PubMed: 29515192]
80. Shambaugh GE, Mrozak SC, Freinkel N (1977) Fetal fuels. I. Utilization of ketones by isolated tissues at various stages of maturation and maternal nutrition during late gestation. Metabolism 26:623–635 [PubMed: 16194]
81. Rinholm JE et al. (2011) Regulation of oligodendrocyte development and myelination by glucose and lactate. J Neurosci 31:538–548 [PubMed: 21228163]
82. Boutrel B, Magistretti PJ (2016) A role for lactate in the consolidation of drug-related associative memories. Biol Psychiatry 79:875–877 [PubMed: 27198521]
83. Newman LA, Korol DL, Gold PE (2011) Lactate produced by glycogenolysis in astrocytes regulates memory processing. PLoS One 6:e28427 [PubMed: 22180782]
84. Gibbs ME, Anderson DG, Hertz L (2006) Inhibition of glycogenolysis in astrocytes interrupts memory consolidation in young chickens. Glia 54:214–222 [PubMed: 16819764]
85. Holmgren CD et al. (2010) Energy substrate availability as a determinant of neuronal resting potential, GABA signaling and spontaneous network activity in the neonatal cortex in vitro. J Neurochem 112:900–912 [PubMed: 19943846]
86. Yang J et al. (2014) Lactate promotes plasticity gene expression by potentiating NMDA signaling in neurons. Proc Natl Acad Sci U S A 111:12228–12233 [PubMed: 25071212]
87. Goyal MS et al. (2014) Aerobic glycolysis in the human brain is associated with development and neotenous gene expression. Cell Metab 19:49–57 [PubMed: 24411938]
88. Sada N et al. (2015) Epilepsy treatment. Targeting LDH enzymes with a stiripentol analog to treat epilepsy. Science 347:1362–1367 [PubMed: 25792327]
89. Leth H et al. (1995) Brain lactate in preterm and growth-retarded neonates. Acta Paediatr 84:495–499 [PubMed: 7633142]
90. Medina JM et al. (1996) Metabolic fuel utilization and pyruvate oxidation during the postnatal period. J Inherit Metab Dis 19:432–442 [PubMed: 8884567]
91. Zhu W et al. (2008) Proton magnetic resonance spectroscopy in neonates with hypoxic-ischemic injury and its prognostic value. Transl Res 152:225–232 [PubMed: 19010293]
92. Wu TW et al. (2018) Cerebral lactate concentration in neonatal hypoxic-ischemic encephalopathy: in relation to time, characteristic of injury, and serum lactate concentration. Front Neurol 9:293 [PubMed: 29867713]
93. Thayyil S et al. (2010) Cerebral magnetic resonance biomarkers in neonatal encephalopathy: a meta-analysis. Pediatrics 125:e382–e395 [PubMed: 20083516]
94. Fink EL et al. (2020) Brain MR imaging and spectroscopy for outcome prognostication after pediatric cardiac arrest. Resuscitation 157:185–194 [PubMed: 32653571]
95. Cady EB et al. (1994) Detection of propan-1,2-diol in neonatal brain by in vivo proton magnetic resonance spectroscopy. Magn Reson Med 32:764–767 [PubMed: 7869898]
96. Pouwels PJW et al. (2019) Spectroscopic detection of brain propylene glycol in neonates: Effects of different pharmaceutical formulations of phenobarbital. J Magn Reson Imaging 49:1062–1068 [PubMed: 30350475]
97. Neale JH, Bzdega T, Wroblewska B (2000) N-Acetylaspartylglutamate: the most abundant peptide neurotransmitter in the mammalian central nervous system. J Neurochem 75:443–452 [PubMed: 10899918]
98. Cangro CB et al. (1987) Immunohistochemistry and biosynthesis of N-acetylaspartylglutamate in spinal sensory ganglia. J Neurochem 49:1579–1588 [PubMed: 2889802]
99. Zhao J et al. (2001) NAAG inhibits KCl-induced [(3)H]-GABA release via mGluR3, cAMP, PKA and L-type calcium conductance. Eur J Neurosci 13:340–346 [PubMed: 11168538]
100. Zuo D et al. (2012) Effects of N-acetylaspartylglutamate (NAAG) peptidase inhibition on release of glutamate and dopamine in prefrontal cortex and nucleus accumbens in phencyclidine model of schizophrenia. J Biol Chem 287:21773–21782 [PubMed: 22570482]

101. Tkac I et al. (2003) Developmental and regional changes in the neurochemical profile of the rat brain determined by in vivo 1H NMR spectroscopy. Magn Reson Med 50:24–32 [PubMed: 12815675]
102. Roller KJ, Coyle JT (1984) Ontogenesis of N-acetyl-aspartate and N-acetyl-aspartyl-glutamate in rat brain. Brain Res 317:137–140 [PubMed: 6467030]
103. Holmes MJ et al. (2017) Longitudinal increases of brain metabolite levels in 5–10 year old children. PLoS One 12:e0180973 [PubMed: 28700727]
104. Wolosker H, D'Aniello A, Snyder SH (2000) D-aspartate disposition in neuronal and endocrine tissues: ontogeny, biosynthesis and release. Neuroscience 100:183–189 [PubMed: 10996468]
105. Hashimoto A et al. (1993) Embryonic development and postnatal changes in free D-aspartate and D-serine in the human prefrontal cortex. J Neurochem 61:348–351 [PubMed: 8515283]
106. D'Aniello G et al. (2007) Reproductive implication of D-aspartic acid in human pre-ovulatory follicular fluid. Hum Reprod 22:3178–3183 [PubMed: 17951582]
107. Errico F et al. (2013) Decreased levels of D-aspartate and NMDA in the prefrontal cortex and striatum of patients with schizophrenia. J Psychiatr Res 47:1432–1437 [PubMed: 23835041]
108. Banay-Schwartz M, Lajtha A, Palkovits M (1989) Changes with aging in the levels of amino acids in rat CNS structural elements. I. Glutamate and related amino acids. Neurochem Res 14:555–562 [PubMed: 2761674]
109. Kornhuber ME et al. (1993) L-glutamate and L-aspartate concentrations in the developing and aging human putamen tissue. J Neural Transm Gen Sect 93:145–150 [PubMed: 8105811]
110. Nuzzo T et al. (2020) Dysfunctional d-aspartate metabolism in BTBR mouse model of idiopathic autism. Biochim Biophys Acta Proteins Proteom 1868:140531 [PubMed: 32853769]
111. Nuzzo T et al. (2017) Decreased free d-aspartate levels are linked to enhanced d-aspartate oxidase activity in the dorsolateral prefrontal cortex of schizophrenia patients. NPJ Schizophr 3:16 [PubMed: 28560262]
112. Kalivas PW (2009) The glutamate homeostasis hypothesis of addiction. Nat Rev Neurosci 10:561–572 [PubMed: 19571793]
113. McKenna MC, Ferreira GC (2016) Enzyme complexes Important for the glutamate-glutamine cycle. Adv Neurobiol 13:59–98 [PubMed: 27885627]
114. Patel AB et al. (2005) The contribution of GABA to glutamate/glutamine cycling and energy metabolism in the rat cortex in vivo. Proc Natl Acad Sci U S A 102:5588–5593 [PubMed: 15809416]
115. Petroff OA (2002) GABA and glutamate in the human brain. Neuroscientist 8:562–573 [PubMed: 12467378]
116. Dwivedi D et al. (2020) Glutathione in brain: overview of its conformations, functions, biochemical characteristics, quantitation and potential therapeutic role in brain disorders. Neurochem Res 45:1461–1480 [PubMed: 32297027]
117. Deoni SC et al. (2011) Mapping infant brain myelination with magnetic resonance imaging. J Neurosci 31:784–791 [PubMed: 21228187]
118. Dydak U et al. (2011) In vivo measurement of brain GABA concentrations by magnetic resonance spectroscopy in smelters occupationally exposed to manganese. Environ Health Perspect 119:219–224 [PubMed: 20876035]
119. Bottomley PA (1987) Spatial localization in NMR spectroscopy in vivo. Ann N Y Acad Sci 508:333–348 [PubMed: 3326459]
120. Scheenen TW et al. (2008) Short echo time 1H-MRSI of the human brain at 3T with minimal chemical shift displacement errors using adiabatic refocusing pulses. Magn Reson Med 59:1–6 [PubMed: 17969076]
121. Andreychenko A et al. (2012) Efficient spectral editing at 7 T: GABA detection with MEGA-sLASER. Magn Reson Med 68:1018–1025 [PubMed: 22213204]
122. Smith MA, Koutcher JA, Zakian KL (2008) J-difference lactate editing at 3.0 Tesla in the presence of strong lipids. J Magn Reson Imaging 28:1492–1498 [PubMed: 19025937]
123. Kelley DA, Wald LL, Star-Lack JM (1999) Lactate detection at 3T: compensating J coupling effects with BASING. J Magn Reson Imaging 9:732–737 [PubMed: 10331771]

124. Abraham D, Pisano JJ, Udenfriend S (1962) The distribution of homocarnosine in mammals. Arch Biochem Biophys 99:210–213 [PubMed: 14010721]
125. Koush Y et al. (2019) Functional MRS with J-edited lactate in human motor cortex at 4T. Neuroimage 184:101–108 [PubMed: 30201463]
126. Liserre R, Pinelli L, Gasparotti R (2021) MR spectroscopy in pediatric neuroradiology. Transl Pediatr 10:1169–1200 [PubMed: 34012861]
127. Terpstra M et al. (2006) Detection of an antioxidant profile in the human brain in vivo via double editing with MEGA-PRESS. Magn Reson Med 56:1192–1199 [PubMed: 17089366]
128. Chan KL, et al. (2017) Simultaneous detection of glutathione and lactate using spectral editing at 3 T. NMR Biomed, 30.
129. Chan KL et al. (2016) HERMES: Hadamard encoding and reconstruction of MEGA-edited spectroscopy. Magn Reson Med 76:11–19 [PubMed: 27089868]
130. Chan KL et al. (2017) Simultaneous measurement of aspartate, NAA, and NAAG using HERMES spectral editing at 3 Tesla. Neuroimage 155:587–593 [PubMed: 28438664]
131. Saleh MG et al. (2016) Simultaneous edited MRS of GABA and glutathione. Neuroimage 142:576–582 [PubMed: 27534734]
132. Oeltzschner G, et al. (2018) Hadamard editing of glutathione and macromolecule-suppressed GABA. NMR Biomed, 31.
133. Saleh MG, et al. (2020) Simultaneous edited MRS of GABA, glutathione, and ethanol. NMR Biomed, 33, e4227. [PubMed: 31943424]
134. Oeltzschner G et al. (2019) Advanced Hadamard-encoded editing of seven low-concentration brain metabolites: principles of HERCULES. Neuroimage 185:181–190 [PubMed: 30296560]
135. Wang ZJ et al. (2008) Brain metabolite levels assessed by lactate-edited MR spectroscopy in premature neonates with and without pentobarbital sedation. AJNR Am J Neuroradiol 29:798–801 [PubMed: 18184837]
136. Ruth L O'Gorman CS, Vera Bernet, Cornelia Hagmann, Martin A. Janich, and Ralph Noeske (2013) LACTATE-EDITED MRS IN NEONATAL HYPOXIC ISCHEMIC ENCEPHALOPATHY. ISMRM.
137. Kwon SH et al. (2014) GABA, resting-state connectivity and the developing brain. Neonatology 106:149–155 [PubMed: 24970028]
138. Xu D et al. (2011) MR spectroscopy of normative premature newborns. J Magn Reson Imaging 33:306–311 [PubMed: 21274971]
139. Waddell KW et al. (2007) A practical guide to robust detection of GABA in human brain by J-difference spectroscopy at 3 T using a standard volume coil. Magn Reson Imaging 25:1032–1038 [PubMed: 17707165]
140. Mullins PG et al. (2014) Current practice in the use of MEGA-PRESS spectroscopy for the detection of GABA. Neuroimage 86:43–52 [PubMed: 23246994]
141. Evans CJ et al. (2013) Subtraction artifacts and frequency (mis-) alignment in J-difference GABA editing. J Magn Reson Imaging 38:970–975 [PubMed: 23188759]
142. Star-Lack J et al. (1998) In vivo lactate editing with simultaneous detection of choline, creatine, NAA, and lipid singlets at 1.5 T using PRESS excitation with applications to the study of brain and head and neck tumors. J Magn Reson 133:243–254 [PubMed: 9716465]
143. Marshall I, Wild JM (1997) Calculations and experimental studies of the lineshape of the lactate doublet in PRESS-localized 1H MRS. Magn Reson Med 38:415–419 [PubMed: 9339443]
144. Lakatos A et al. (2019) Neurodevelopmental effect of intracranial hemorrhage observed in hypoxic ischemic brain injury in hypothermia-treated asphyxiated neonates - an MRI study. BMC Pediatr 19:430 [PubMed: 31718607]
145. Choi IY et al. (2021) Spectral editing in (1) H magnetic resonance spectroscopy Experts consensus recommendations. NMR Biomed 34:e4411 [PubMed: 32946145]
146. Raschle NM, et al. (2009) Making MR imaging child's play - pediatric neuroimaging protocol, guidelines and procedure. J Vis Exp.
147. Tisdall MD et al. (2012) Volumetric navigators for prospective motion correction and selective reacquisition in neuroanatomical MRI. Magn Reson Med 68:389–399 [PubMed: 22213578]

148. Hess AT et al. (2011) Real-time motion and B0 corrected single voxel spectroscopy using volumetric navigators. Magn Reson Med 66:314–323 [PubMed: 21381101]

149. Wilson M et al. (2019) Methodological consensus on clinical proton MRS of the brain: review and recommendations. Magn Reson Med 82:527–550 [PubMed: 30919510]

150. Cady EB (1996) Metabolite concentrations and relaxation in perinatal cerebral hypoxic-ischemic injury. Neurochem Res 21:1043–1052 [PubMed: 8897467]

151. Cheong JL et al. (2006) Proton MR spectroscopy in neonates with perinatal cerebral hypoxic-ischemic injury: metabolite peak-area ratios, relaxation times, and absolute concentrations. AJNR Am J Neuroradiol 27:1546–1554 [PubMed: 16908578]

152. Cady EB et al. (1996) Lactate, N-acetylaspartate, choline and creatine concentrations, and spin-spin relaxation in thalamic and occipito-parietal regions of developing human brain. Magn Reson Med 36:878–886 [PubMed: 8946353]

153. Kreis R, Ernst T, Ross BD (1993) Development of the human brain: in vivo quantification of metabolite and water content with proton magnetic resonance spectroscopy. Magn Reson Med 30:424–437 [PubMed: 8255190]

154. Holland BA et al. (1986) MRI of normal brain maturation. AJNR Am J Neuroradiol 7:201–208 [PubMed: 3082150]

155. Deoni SC et al. (2012) Investigating white matter development in infancy and early childhood using myelin water faction and relaxation time mapping. Neuroimage 63:1038–1053 [PubMed: 22884937]

156. Melbourne A et al. (2016) Longitudinal development in the preterm thalamus and posterior white matter: MRI correlations between diffusion weighted imaging and T2 relaxometry. Hum Brain Mapp 37:2479–2492 [PubMed: 26996400]

157. Kulpanovich AA, Tal A (2018) The application of magnetic resonance fingerprinting to single voxel proton spectroscopy. NMR Biomed 31:e4001 [PubMed: 30176091]

158. Kirov II, Tal A (2020) Potential clinical impact of multiparametric quantitative MR spectroscopy in neurological disorders: a review and analysis. Magn Reson Med 83:22–44 [PubMed: 31393032]

159. Maenner MJ et al. (2020) Prevalence of autism spectrum disorder among children aged 8 years - autism and developmental disabilities monitoring network, 11 sites, United States, 2016. MMWR Surveill Summ 69:1–12

160. Kim H et al. (2016) Estimating epilepsy incidence and prevalence in the US pediatric population using nationwide health insurance claims data. J Child Neurol 31:743–749 [PubMed: 26719495]

161. Brown RT et al. (2001) Prevalence and assessment of attention-deficit/hyperactivity disorder in primary care settings. Pediatrics 107:E43 [PubMed: 11230624]

162. Thayyil S (2019) Cooling therapy for the management of hypoxic-ischaemic encephalopathy in middle-income countries: we can, but should we? Paediatr Int Child Health 39:231–233 [PubMed: 30938237]

163. Juul SE et al. (2018) High-dose erythropoietin for asphyxia and encephalopathy (HEAL): a randomized controlled trial - background, aims, and study protocol. Neonatol 113:331–338

164. Lally PJ et al. (2019) Magnetic resonance spectroscopy assessment of brain injury after moderate hypothermia in neonatal encephalopathy: a prospective multicentre cohort study. Lancet Neurol 18:35–45 [PubMed: 30447969]

165. Jordan CJ, et al. (2020) Introduction to the Special Issue on “Informing Longitudinal Studies on the Effects of Maternal Stress and Substance Use on Child Development: Planning for the HEALthy Brain and Child Development (HBCD) Study”. Advers Resil Sci, 1–5. [PubMed: 33106790]

166. Volkow ND, Gordon JA, Freund MP (2021) The healthy brain and child development study-shedding light on opioid exposure, COVID-19, and health disparities. JAMA Psychiat 78:471–472

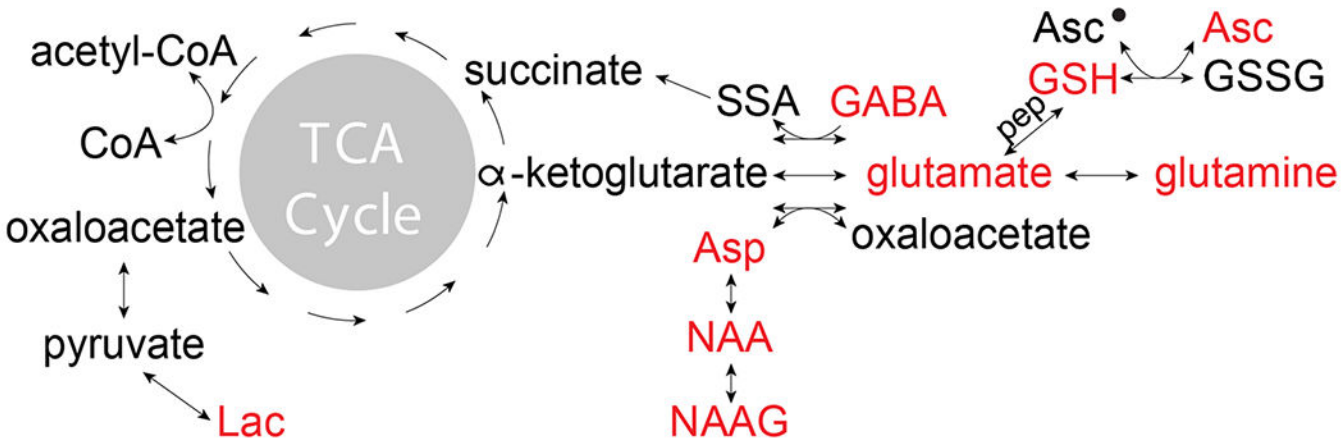

Fig. 1.

Pathways relating the editable metabolites in the human brain. Abbreviations: TCA, tricarboxylic acid cycle; SSA, succinic semialdehyde; Asp, aspartate; Asc, ascorbate; GABA, γ-aminobutyric acid; NAA, N-acetylaspartate; NAAG, N-acetyl-aspartylglutamate

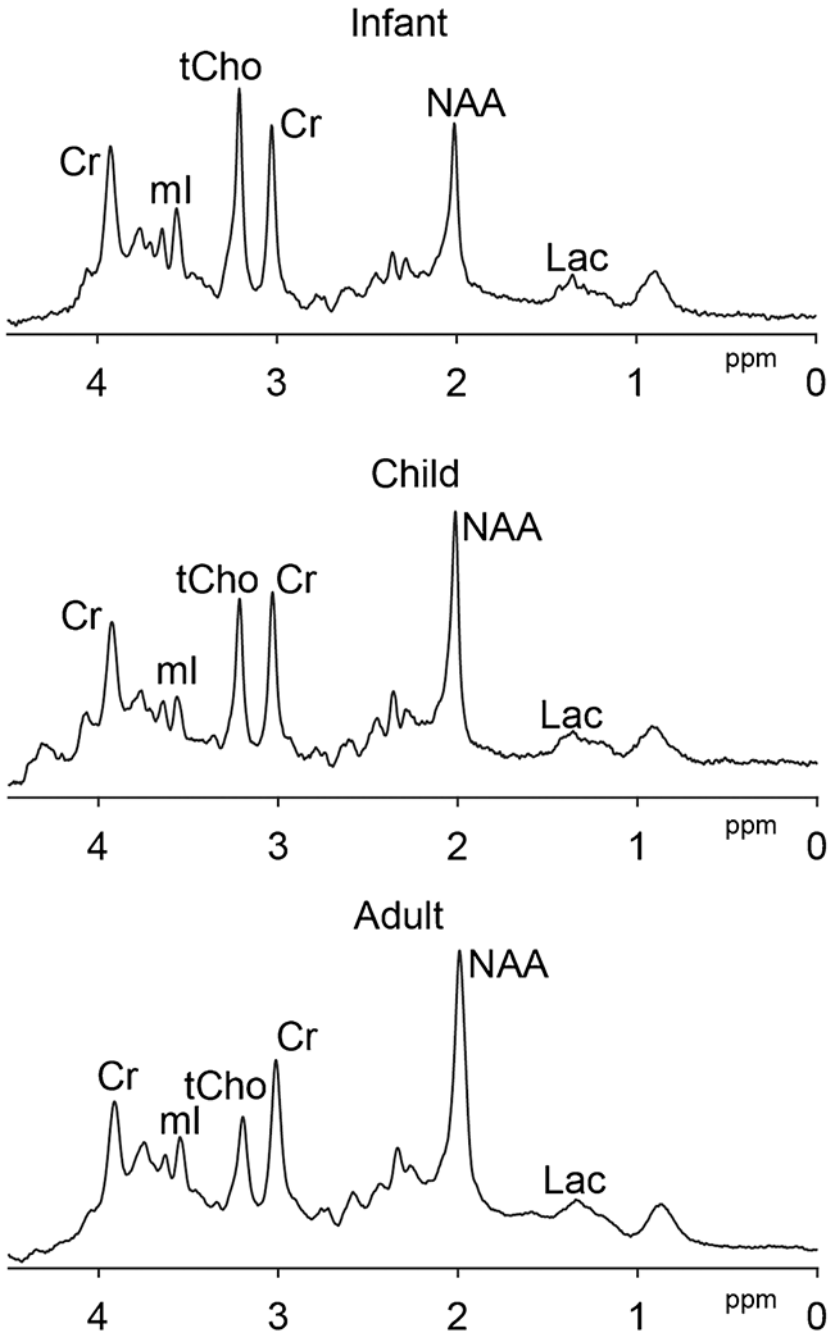

Fig. 2.

Age-related change of the proton MRS brain spectra at 3 T. Infant (GA at birth, 36w; scanned at 38 weeks 6 days; volume = 24 × 40 × 24mm^3 in bilateral thalamus, TE = 35 ms, average = 64), child (4-year-old, volume = 17 × 40 × 17mm^3 in bilateral thalamus, TE = 35 ms, average = 32), adult (24-year-old, volume = 30 × 30 × 30mm^3 in posterior cingulate, TE = 35 ms, average =64) short-TE PRESS spectra with TR = 2 s are shown, respectively. Spectra are normalized to the Cr signal amplitude. tCho, NAA, and Lac levels can be seen to change with age, as does the linewidth

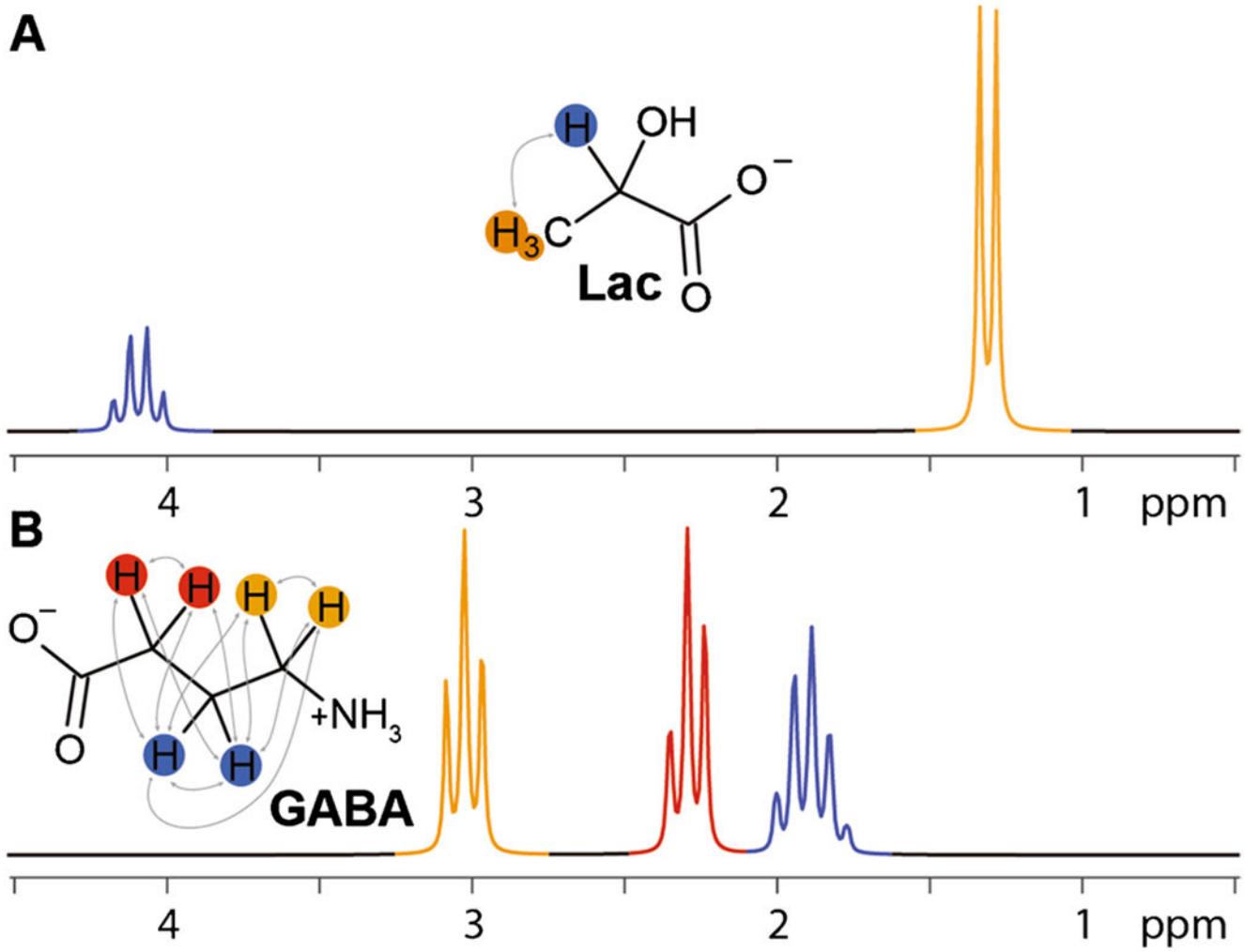

Fig. 3.

J-coupling. J-couplings of lactate (**A**) and GABA (**B**) are superimposed on the molecular structures as gray arrows. These result in the multiplet splittings seen in the simulated MR spectra below

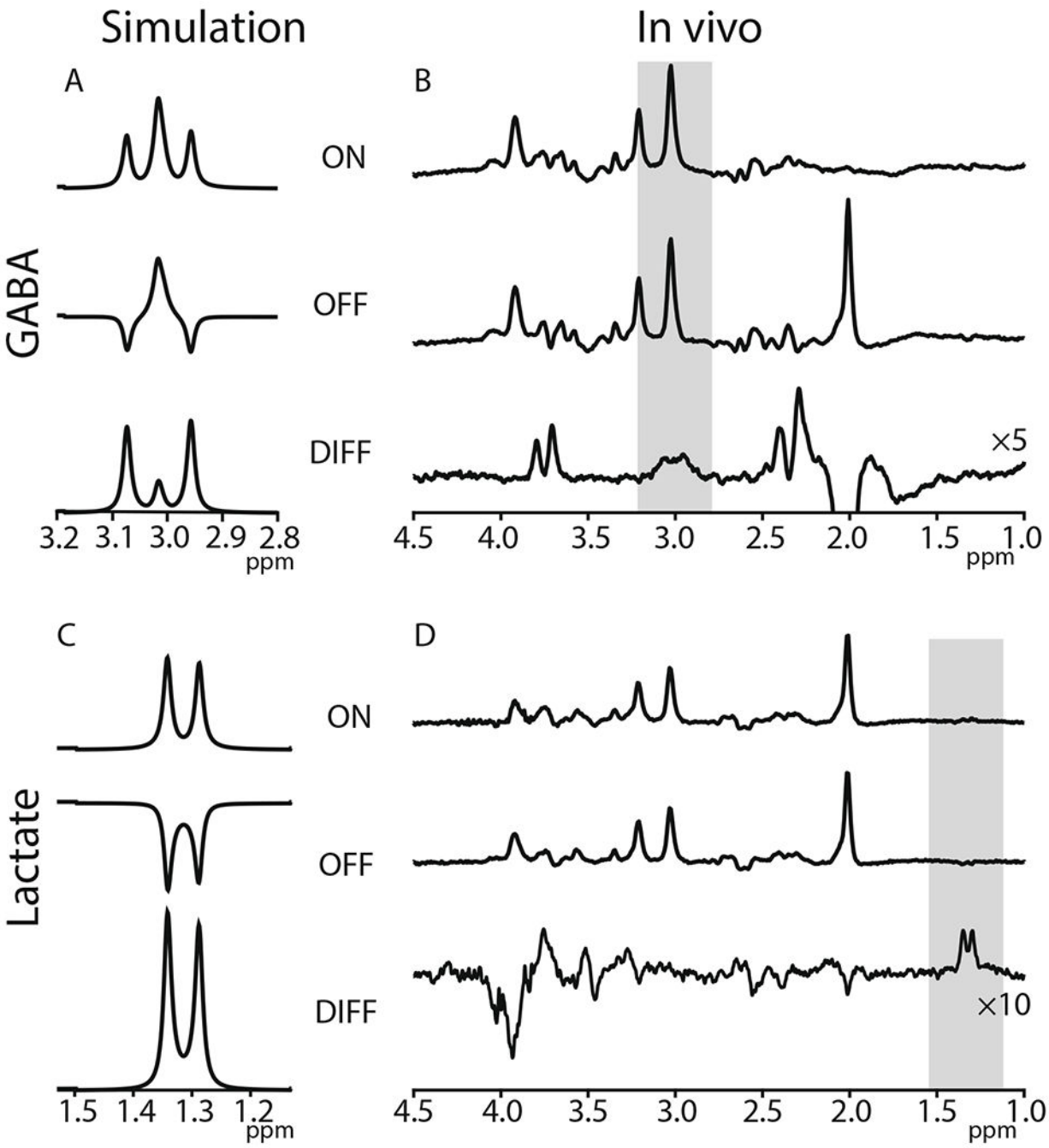

Fig. 4.

J-difference editing of GABA and lactate. GABA-edited spectra in simulation (**A**) and in vivo (**B**). The shaded region marks the edited GABA signal at 3 ppm. Lac-edited spectra in simulation (**C**) and in vivo (**D**). The shaded region marks the edited Lac signal at 1.3 ppm. Simulation sequence parameter: GABA: TE = 80 ms, field strength = 3 T; Lac: TE = 140 ms, field strength = 3 T. In vivo sequence parameter: GABA: TR = 2 s, TE = 80 ms, field strength = 3 T, averages = 320, acquisition bandwidth = 2000 Hz, acquisition time: 10

min 40 s; Lac: TR = 2 s, TE = 140 ms, field strength = 3 T, averages = 320, acquisition bandwidth = 2000 Hz, acquisition time: 10 min 40 s

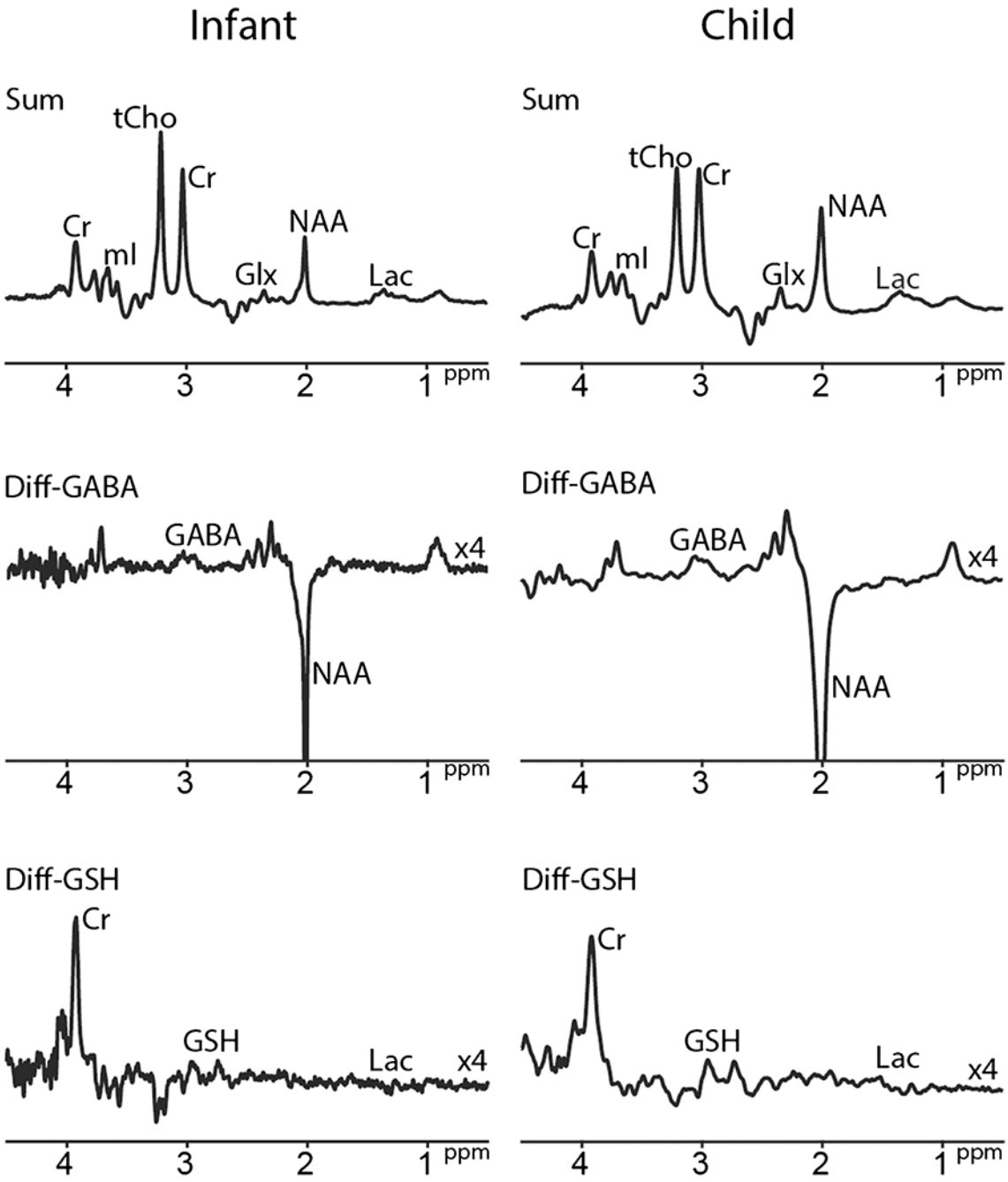

Fig. 5.

HERCULES-edited spectra in infant and child at 3 T. Infant (GA at birth, 36w; scanned at 38 weeks 6 days; volume = 17 × 40 × 17mm^3 in bilateral thalamus, TE = 80 ms. Average = 56), child (4-year-old, volume = 24 × 40 × 24mm^3 in bilateral thalamus, TE = 80 ms, average = 56) HERCULES spectra with TR = 2 s are shown, respectively. Spectra are normalized to the Cr signal amplitude. Y-scaling of difference spectra is increased by a factor of 4. Abbreviations: tCr, total creatine; tCho, total choline; mI, myo-inositol; Glx, glutamate + glutamine; tNAA, total N-acetyl aspartate; Lac, lactate; MM,

macromolecule; GABA, γ-aminobutyric acid; Asc, ascorbate; PE, phosphorylethanolamine; GSH, glutathione; Asp, aspartate; NAAG, N-acetylaspartylglutamate

Table 1

Concentration ranges for editable metabolites, as reported for healthy adult and infant human brain and biopsy tissues, using various techniques (including MRS). Augmented from [36]. Note that the units, correction factors, and assumptions underlying MRS quantification vary between studies and may not be directly comparable

Metabolites	Adults		Neonates	
	Concentration range	References	Concentration range	References
GABA	1.3–1.9 mmol/kg_{ww}	[37, 38]	~ 1.0 i.u*	[39–41]
GSH	2.0 mmol/kg_{ww}	[42]	2.5 mmol/kg_{ww}	[3]
Ascorbate	1.1–1.3 mmol/kg_{ww}	[43, 44]	-	-
Lactate	0.4 mmol/kg_{ww}	[38]	0.8 mmol/kg_{ww}	[3]
NAAG	0.6–2.7 mmol/kg_{ww}	[45]	0.9 mmol/kg_{ww}	[3]
Aspartate	1.0–1.4 mmol/kg_{ww}	[37, 42]	3.0 mmol/kg_{ww}	[3]

*Based upon several studies with inconsistent brain regions and quantification approaches.

Table 2

Summary of advantages and disadvantages of different approaches to in vivo edited MRS

Name	Advantages	Disadvantages	Has been used in neonates	References
J-difference editing	Reliable quantification of the low-concentration metabolites	One ROI and one metabolite-of-interest per experiment	Yes	[39, 40, 57, 135–137]
Advanced editing	Simultaneous acquisition of multiple metabolites in one experiment	Increased sensitivity to motion and B_0 instabilities	Yes	[41]
MRSI	Spatial mapping of metabolite levels	High sensitivity to motion, long scan time, and complex post-processing	Yes	[16, 138]

Table 3

In vivo applications of edited MRS in neonates. Methods and major findings are summarized.

Ref	Method	B_0 (T)	Volume (cm^3)	TR/TE (ms)	Duration (min)	Regions	Sedation	Findings	Subject number	Age range (GA weeks w)
[135]	Edited-Lac 3D MRS	1.5	1 (8 × 8 × 8 array)	2000/144	17.5	Right BG, Thal, CS	Yes & No	BG Lac lower in sedated neonates	43 preterm	< 34w
[136]	BASING	3	3.4 or 4.1	3000/144	-	Left BG	-	Editing improves specificity/ reliability of Lac detection in neonates	5 infants	-
[137]	MEGA-PRESS	3	18	1500/68	20	Right frontal lobe	No	GABA levels in preterm infants < term infants	18 preterm & 21 term	Preterm: mean: (27w) Term:37–41w(40w)
[40]	MEGA-PRESS	3	15.6	1500/68	6.9	Right BG	Yes	No change in GABA between 37–46w PMA and 64–73w	20 preterm	< 34 w
[57]	MEGA-PRESS	3	Neonate: 4–9 Children: 13–37	1500/69	3.2	Left BG, cerebellum	Yes	Lower GABA levels in neonates than children	38 neonates & 12 children	Neonates (preterm: 23–36w; term: 37–41w) Children: 6–16 years
[39]	MEGA-PRESS	3	4.5	2000/68	8.5	Right frontal lobe	No	Correlations between GABA and GA (−ve) and postnatal age (+ve). Higher GABA at TEA in those born < 28 w	38 preterm	< 32w, median 28w
[41]	HERMES	3	15.6	2000/80	10.6	Left Thal, ACC	No	Differences in GABA + and Glu, (not GSH) between regions	18 neonates	29–41w

Abbreviations: *BG* basal ganglia, *ACC* anterior cingulate, *Thal* thalamus, *CS* centrum semiovale, *GA* gestational age, *PMA* postmenstrual age, *TEA* term-equivalent age, *w* weeks

Table 4

Metabolite relaxation times of NAA, creatine and choline methyl singlet groups at 2.0 ppm, 3.0 ppm, and 3.2 ppm, respectively, reported in normal neonates at different fields. All data are given in milliseconds (mean ± SD).

Region	B_0 (T)	Ref	T_1 (ms)					T_2 (ms)					Age (GA w)
			NAA	Cr	Cho	mI	Lac	NAA	Cr	Cho	mI	Lac	
Occ GM	1.5	[153]	930 ± 476	1620 ± 529	1320 ± 370	1520 ± 529	-	524 ± 207	228 ± 29	431 ± 98	301 ± 66	-	T_1: 41 ± 1 T_2: 42 ± 3
Occ WM	2.4	[152]	1220 ± 280[a]	1600 ± 700[a]	1130 ± 220[a]	-	1230 ± 420[a]	463.5 ± 129.6	198.4 ± 42.3	498.4 ± 239.7	-	241.9 ± 119.9	T_1: N/A; T_2: 35.2 (mean)
Thal	2.4	[151]	1310 ± 310	1660 ± 640	1180 ± 220	-	1280 ± 440	638.9 ± 68.1	199.2(192.4–225.3)	383.6 ± 84.2	-	221.8(196.3–287.7)	39 ± 1.8
Thal	2.4	[150]	-	-	-	-	-	316.3 ± 78.4	209.1 ± 35.8	327.8 ± 87.5	-	231.5 ± 53.5	32–42 (range)
Thal	2.4	[152]	1220 ± 280	1600 ± 700	1130 ± 220	-	1230 ± 420	331 ± 90.6	204 ± 35.2	343.7 ± 99.9	-	244.4 ± 107.1	T_1: N/A; T_2: 35.2 (mean)
Thal	3	[76]	1410 ± 220	1600 ± 200	1150 ± 180	-	-	480 ± 100	205 ± 17	430 ± 70	-	-	40 ± 2

Abbreviations: *Occ* Occipital, *Thal* thalamus, *GM* gray matter, *WM* white matter, *NAA* N-acetylaspartate, *Cr* creatine, *Cho* choline, *mI* myo-inositol, *Lac* lactate, *w* week, *GA* gestational age.

[a] T_1 estimates were only reported for the Thalamus but found to be similar in Occ